ULTRASOUND NEWS

July, 2023

Kaeley et al. Arthritis Research & Therapy (2020) 22:1
https://doi.org/10.1186/s13075-019-2050-4

Arthritis Research & Therapy

REVIEW Open Access

The importance of ultrasound in identifying and differentiating patients with early inflammatory arthritis: a narrative review

Gurjit S. Kaeley[1*], Catherine Bakewell[2] and Atul Deodhar[3]

Abstract

Early differentiation between different types of inflammatory arthritis and subsequent initiation of modern treatments can improve patient outcomes by reducing disease activity and preventing joint damage. Routine clinical evaluation, laboratory testing, and radiographs are typically sufficient for differentiating between inflammatory and predominantly degenerative arthritis (e.g., osteoarthritis). However, in some patients with inflammatory arthritis, these techniques fail to accurately identify the type of early-stage disease. Further evaluation by ultrasound imaging can delineate the inflammatory arthritis phenotype present. Ultrasound is a noninvasive, cost-effective method that enables the evaluation of several joints at the same time, including functional assessments. Further, ultrasound can visualize pathophysiological changes such as synovitis, tenosynovitis, enthesitis, bone erosions, and crystal deposits at a subclinical level, which makes it an effective technique to identify and differentiate most common types of inflammatory arthritis. Limitations associated with ultrasound imaging should be considered for its use in the differentiation and diagnosis of inflammatory arthritides.

Keywords: Ultrasound, Inflammatory arthritis, Synovitis, Enthesitis, Bone erosions, Imaging

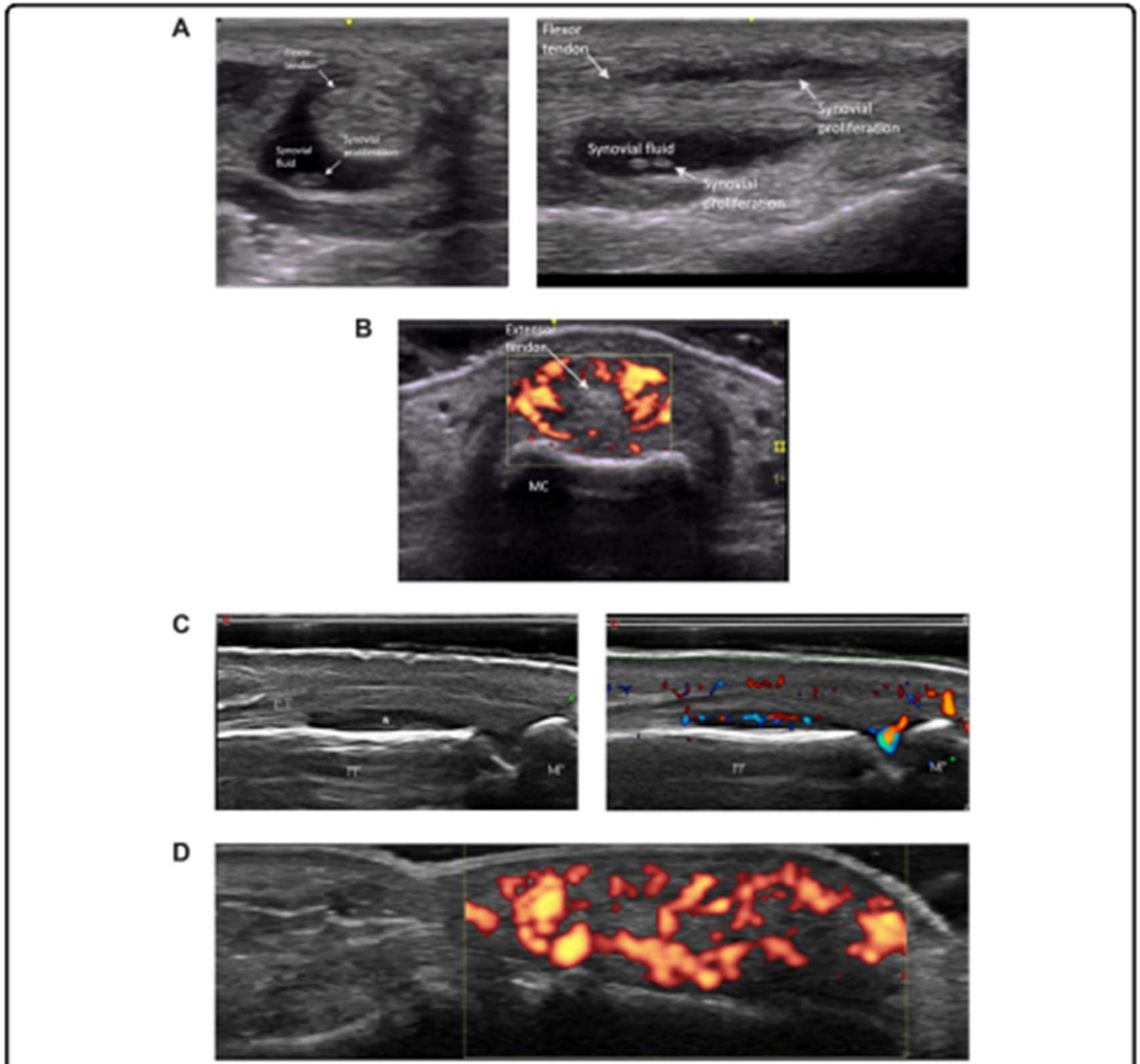

Fig. 2 Ultrasound imaging of synovitis and tenosynovitis. a Flexor tenosynovitis in transverse (left) and longitudinal (right) views. b Metacarpophalangeal joint paratenonitis, dorsal aspect of second metacarpophalangeal joint. MC, metacarpal. c Dorsal proximal interphalangeal B-mode (left) and power Doppler (right) images indicating synovitis in the recess (asterisk). PP, proximal phalanx; MP, middle phalanx; ET, extensor digitorum tendon. d Positive power Doppler signal of finger pulp

findings for differentiation of psoriatic arthritis
arthritis. **a** Short-axis view of palmar plate
flexor tendon; MH, metacarpal head; PP, palmar
ng view of enthesitis of the extensor tendon from
ngeal joint in a patient with psoriatic arthritis.
alangeal; S, DIP synovitis; asterisk (*), enthesophyte;
**), extensor tendon demonstrating thickening,
, and loss of fibrillar architecture; triple asterisks
don with insertional Doppler

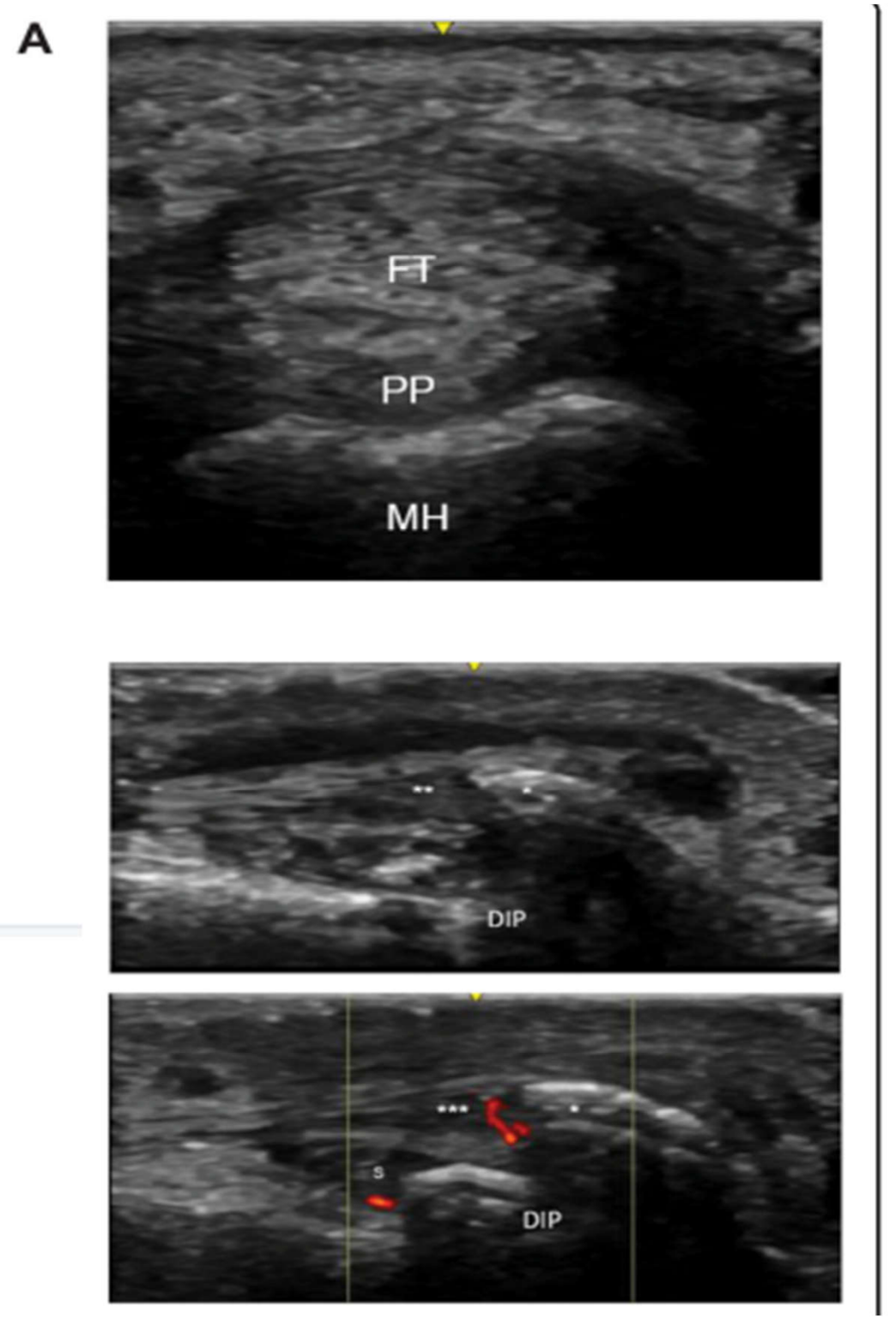

rch Article

sound Assessment of Synovial Thickness of Some of Metacarpophalangeal Joints of Hand in matoid Arthritis Patients and the Normal Population

Zuhudha Hussain Manik,[1] John George,[1] and Sargunan Sockalingam[2]

University of Malaya Research Imaging Centre, Faculty of Medicine, University of Malaya, Kuala Lumpur, Malaysia
Department of Medicine, Faculty of Medicine, University of Malaya, Kuala Lumpur, Malaysia

Correspondence should be addressed to Zuhudha Hussain Manik; xuhudha@gmail.com

Received 28 December 2015; Revised 16 March 2016; Accepted 20 March 2016

Academic Editor: Giuseppe Murdaca

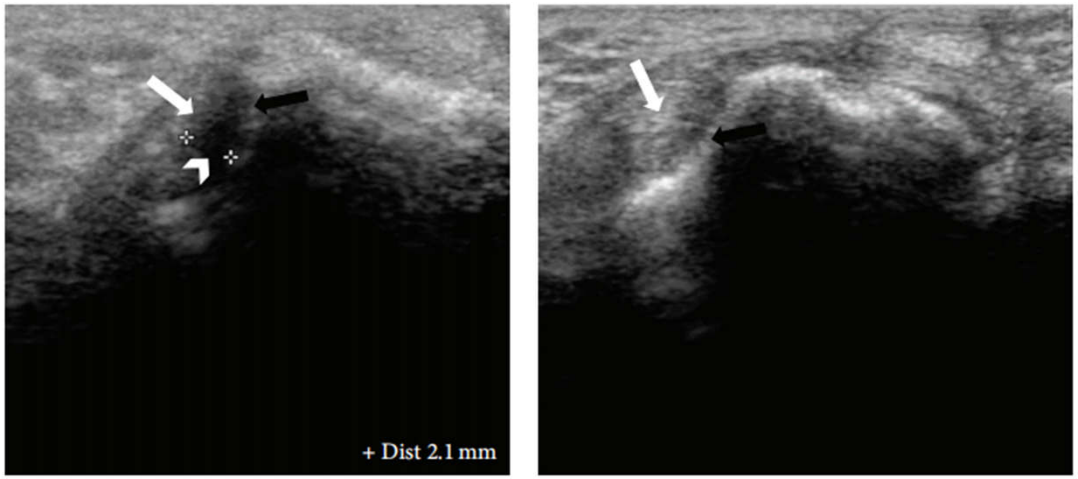

(a) (b)

FIGURE 2: Dorsal ultrasound images of MCPJ at bare areas. (a) Radial recess shows distinct hypoechoic synovium (*arrow head*) compared to displaced hyperechoic proper collateral ligament (*white arrow*) and bone (*black arrow*). Calipers are being used to measure the maximal synovial thickness at this region with characteristic appearance on ultrasound. (b) shows no synovial thickening between the proper collateral ligament (white arrow) and adjacent to cortical bone (*black arrow*).

FIGURE 1: Position for examination of the hands. The neutral dorsal transverse position of the transducer in line with the radial and ulnar bare area of the metacarpophalangeal joint.

NAL ARTICLE

oring ultrasound synovitis in eumatoid arthritis: a EULAR-MERACT ultrasound taskforce— rt 1: definition and development a standardised, consensus-based oring system

a-Antonietta D'Agostino,[1,2] Lene Terslev,[3] Philippe Aegerter,[4,5] na Backhaus,[6] Peter Balint,[7] George A Bruyn,[8] Emilio Filippucci,[9] er Grassi,[9] Annamaria Iagnocco,[10] Sandrine Jousse-Joulin,[11,12] d Kane,[13] Esperanza Naredo,[14] Wolfgang Schmidt,[15] Marcin Szkudlarek,[16] o G Conaghan,[17] Richard J Wakefield[17]

schematic drawing of the individual grades of hypoechoic SH for GS alone. For each onding GS image. (1) None=Grade 0: no SH independently of the presence of effusion; without effusion up to level of horizontal line connecting bone surfaces M and P; (3) without effusion extending beyond joint line but with upper surface convex (curved downwards) d joint line but with upper surface flat; (4) severe=Grade 3: SH with or without effusion with upper surface flat or convex (curved downwards). Panel 2b shows the schematic drawing pler activity. For each grade is also shown the corresponding ultrasound image. (1) None=Grade al=Grade 1: up to three single Doppler spots or up to one confluent spot and two single ots; (3) moderate=Grade 2: greater than Grade 1 but <50% Doppler signals in the total GS : greater than Grade 2 (>50% of the background GS). Panel 2c shows the EULAR-OMERACT ning grey-scale SH and PD signal. Normal joint=Grade 0: no grey-scale-detected SH and no minimal synovitis=Grade 1: Grade 1 SH and ≤Grade 1 PD signal; moderate synovitis=Grade signal or Grade 1 SH *and* a Grade 2 PD signal; severe synovitis=Grade 3: Grade 3 SH and or 2 synovial hypertrophy *and* a Grade 3 PD signal. fx1, connective tissue; EULAR, European S, grey-scale; fx2, hypertrophy; fx3, joint line; fx4, loose intra-articular connective tissue; M, alangeal bone; OMERACT, Outcome Measures in Rheumatology; PD, power Doppler; SH,

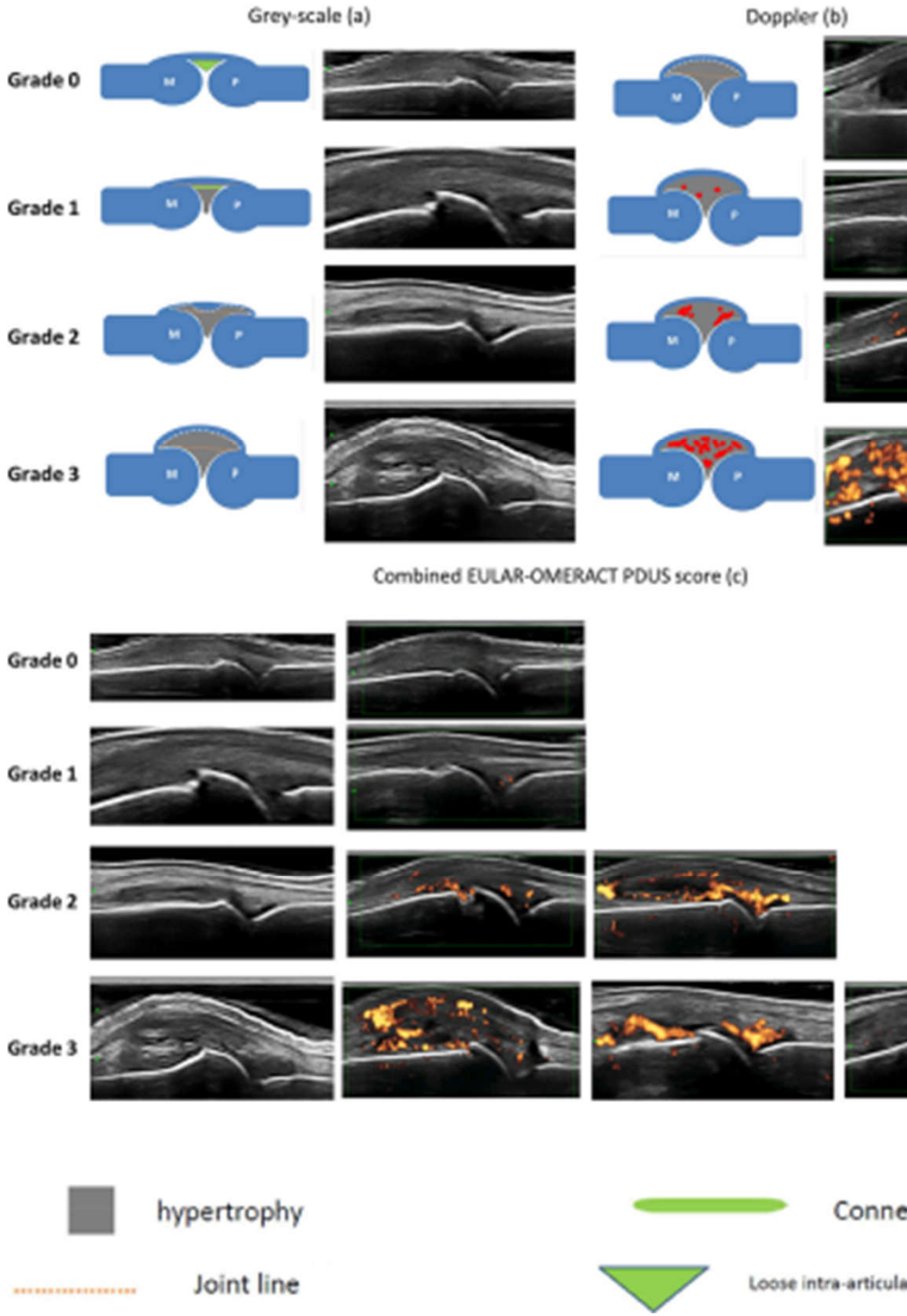

ORIGINAL ARTICLE

Scoring ultrasound synovitis in rheumatoid arthritis: a EULAR-OMERACT ultrasound taskforce-Part 2: reliability and application to multiple joints of a standardised consensus-based scoring system

Lene Terslev,[1] Esperanza Naredo,[2] Philippe Aegerter,[3] Richard J Wakefield,[4] Marina Backhaus,[5] Peter Balint,[6] George A W Bruyn,[7] Annamaria Iagnocco,[8] Sandrine Jousse-Joulin,[9] Wolfgang A Schmidt,[10] Marcin Szkudlarek,[11] Philip G Conaghan,[4] Emilio Filippucci,[12] Maria Antonietta D'Agostino[13,14]

Conclusion The EULAR-OMERAC
demonstrated moderate-good rel
MCP joints using a standardised s
equally applicable in non-MCP joi
scoring system should underpin ir
reliability and consequently the re
of US in RA clinical trials.

test the reliability of new ultrasound (US) definitions and quantification of synovial hypertrophy (SH) and power Doppler (PD)
ation, in a range of joints in patients with rheumatoid arthritis (RA) using the European League Against Rheumatisms–Outcom
(EULAR-OMERACT) combined score for PD and SH.
epwise approach was used: (1) scoring static images of metacarpophalangeal (MCP) joints in a web-based exercise and subseq
nts; (2) scoring static images of wrist, proximal interphalangeal joints, knee and metatarsophalangeal joints in a web-based ex
when scanning patients using different acquisitions (standardised vs usual practice). For reliability, kappa coefficients (κ) were

g MCP joints in static images showed substantial intraobserver variability but good to excellent interobserver reliability. In pati
the same for the two acquisition methods. Interobserver reliability for SH (κ=0.87) and PD (κ=0.79) and the EULAR-OMERACT
better when using a 'standardised' scan. For the other joints, the intraobserver reliability was excellent in static images for all
bserver reliability marginally lower. When using standardised scanning in patients, the intraobserver was good (κ=0.64 for SH
nbined score, 0.66 for PD) and the interobserver reliability was also good especially for PD (κ range=0.41–0.92).

dical Ultrasonics > Article

nterology | Published: 18 February 2023

of strain elastography and shear wave
in diagnosis of fibrosis in nonalcoholic
ease

ui, Hidenari Nagai & Takahisa Matsuda

onics **50**, 187–195 (2023) | Cite this article

ions | Metrics

Results

In total, 107 patients (65 men, 42 women; mean age 51 ± 14 y analyzed. The S-Map value by fibrosis stage was 34.4 ± 10.9 fo for F1, 29.5 ± 5.6 for F2, 26.7 ± 6.0 for F3, and 22.8 ± 4.19 for stage, the SWE value was 1.27 ± 0.25 for F0, 1.39 ± 0.20 for F1 for F2, 1.64 ± 0.17 for F3, and 1.88 ± 0.19 for F4. The diagnost of S-Map (measured by area under the curve) was 0.75 for F2 and 0.85 for F4. The diagnostic performance of SWE (measure under the curve) was 0.88 for F2, 0.87 for F3, and 0.92 for F4.

Conclusion

S-Map strain elastography was inferior to terms of ability to diagnose fibrosis in NA

bility of S-Map strain elastography to diagnose fibrosis in nonalcoholic fatty liver disease (NAFLD) e its diagnostic ability with that of shear wave elastography (SWE).

ere patients with NAFLD who were scheduled to undergo liver biopsy at our institution between 9. A GE Healthcare LOGIQ E9 ultrasound system was used. For S-Map, the right lobe of the liver wa he section where the heartbeat was detected by right intercostal scanning, a 4 × 2-cm region of was defined at 5 cm from the liver surface, and ROI strain images were acquired. Measurements six times, with the average taken as the S-Map value. Correlations of S-Map and SWE values with determined by liver biopsy were analyzed using multiple comparisons. The diagnostic performance osis staging was assessed using receiver operating characteristic curves.

ors affecting testicular volume after iopexy for undescended testes

jiki, Tsukasa Narukawa ... Osamu Ukimura

nal Article–Urology

shed: 12 June 2023

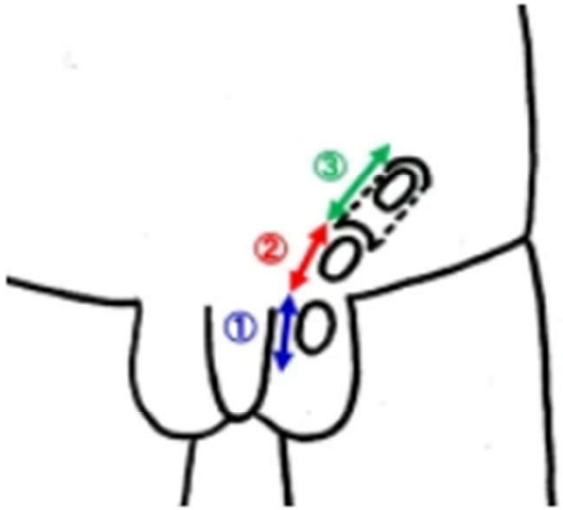

①Upper scrotu
:The operations we
scrotal approach.
②Inguinal exte
:The operations
by Inguinal externa
③Inguinal cana
: The operations
by inguinal approa

All of them wer
according to intraop

usion

orchiopexy TA may occur regardless of the patient's age at orchiopexy, and orchiopexy is
mmended irrespective of age at diagnosis.

Features of ductal carcinoma in situ ultrasound images

Takanori Watanabe

Special Feature: Review Article

Open Access | Published: 28 June 2023

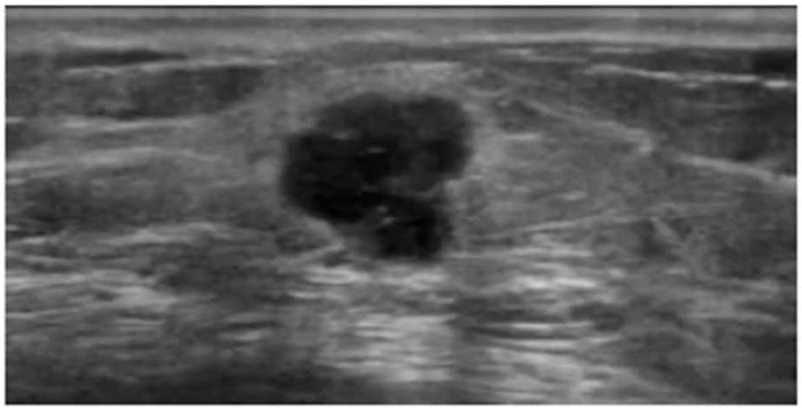

Abstract

Ultrasound images of ductal carcinoma in situ (DCIS) show a wide range of variations from mass to non-mass lesions. This article describes the characteristics of ultrasound images of DCIS based on the BC-02 study conducted by The Japanese Association of Breast and Thyroid Sonology (JABTS). In the BC-02 study, ultrasound images of 705 DCIS cases were classified by imaging findings. The results showed that non-mass abnormalities accounted for 60% of all lesions and masses for 40%. Looking at each subclassification, hypoechoic areas in the mammary gland were the most common (50% of the total), followed by solid masses (31%), mixed masses (9%), and abnormalities of the ducts (8%). These four classifications accounted for 98% of the total. Echogenic foci without a hypoechoic area, architectural distortion, and clustered microcysts were very rare, accounting for about 1% of the total. The ultrasound images of DCIS were characterized by a wide range of variations from masses to non-masses abnormalities, with hypoechoic areas in the mammary gland being the most common, followed by solid masses.

Abu-Zidan and Cevik *World Journal of Emergency Surgery* (2018) 13:47
https://doi.org/10.1186/s13017-018-0209-y

World Journal of Emergency Surgery

REVIEW Open Access

Diagnostic point-of-care ultrasound (POCUS) for gastrointestinal pathology: state of the art from basics to advanced

Fikri M Abu-Zidan[1*] and Arif Alper Cevik[2]

Abstract

The use of point-of-care ultrasound (POCUS) by non-radiologists has dramatically increased. POCUS is completely different from the routine radiological studies. POCUS is a Physiological, On spot, extension of the Clinical examination, that is Unique, and Safe. This review aims to lay the basic principles of using POCUS in diagnosing intestinal pathologies so as to encourage acute care physicians to learn and master this important tool. It will be a useful primer for clinicians who want to introduce POCUS into their clinical practice. It will cover the basic physics, technical aspects, and simple applications including detection of free fluid, free intraperitoneal air, and bowel obstruction followed by specific POCUS findings of the most common intestinal pathologies encountered by acute care physicians including acute appendicitis, epiploic appendagitis, acute diverticulitis, pseudomembranous colitis, intestinal tuberculosis, Crohn's disease, and colonic tumours. Deep understanding of the basic physics of ultrasound and its artefacts is the first step in mastering POCUS. This helps reaching an accurate POCUS diagnosis and avoiding its pitfalls. With increased skills, detailed and accurate POCUS findings of specific intestinal pathologies can be achieved and properly correlated with the clinical picture. We have personally experienced and enjoyed this approach to a stage that an ultrasound machine is always accompanying us in our clinical on calls and rounds.

Keywords: Ultrasound, Point-of-care, Basic physics, Bowel obstruction, Bowel perforation, Free fluid, Appendicitis, Diverticulitis, Tumour, Intestine, Inflammation, Tuberculosis

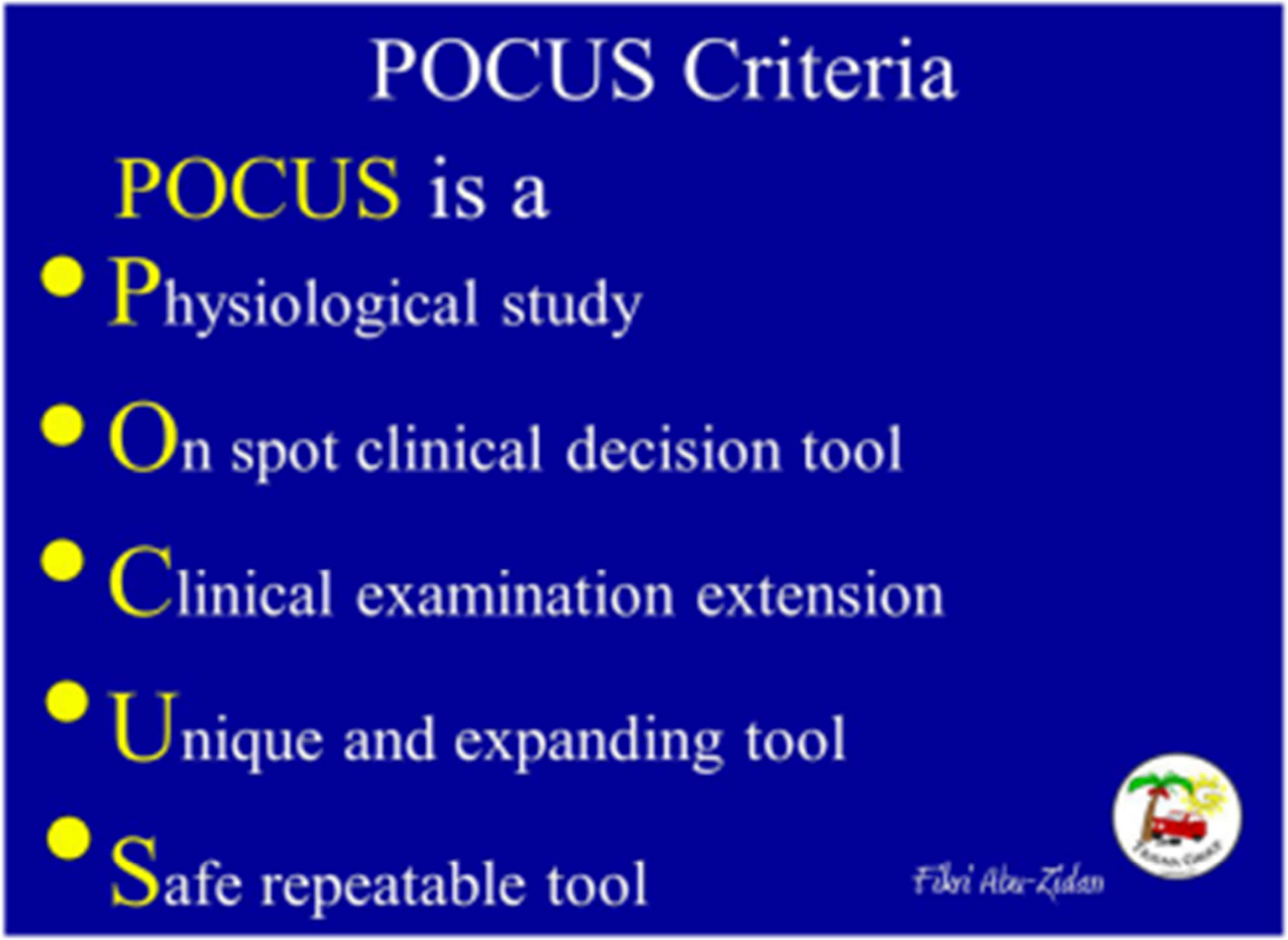

Fig. 1 Major characteristics of point-of-care ultrasound (POCUS) which is performed by acute care physicians and makes it different from routine ultrasound examinations

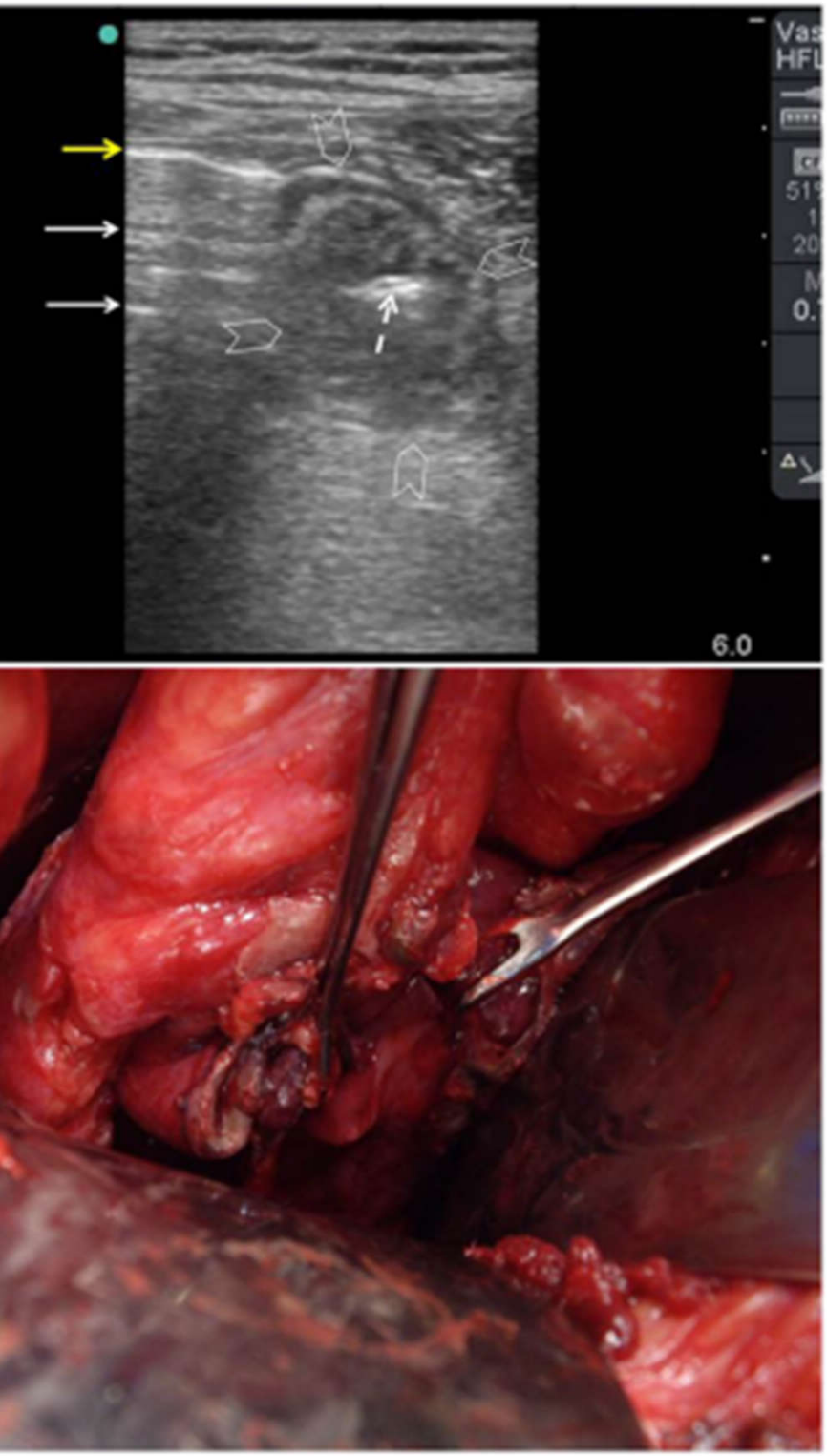

Fig. 5 A 45-year-old man presented with suprapubic pa
dysuria. Abdominal examination showed guarding and
in the suprapubic region. POCUS using a high-frequenc
probe (**a**) showed thickened inflamed small bowel (arro
having gas within it (white dashed arrow). The significa
intra-peritoneal air was seen as an "enhanced peritonea
which is the hyperechoic white line located just under
abdominal fascia (yellow arrow). The reverberation lines
arrows) represent the repetition of the reflective waves.
examination detected a large self-inflicted rectal tear. La
confirmed the findings (**b**)

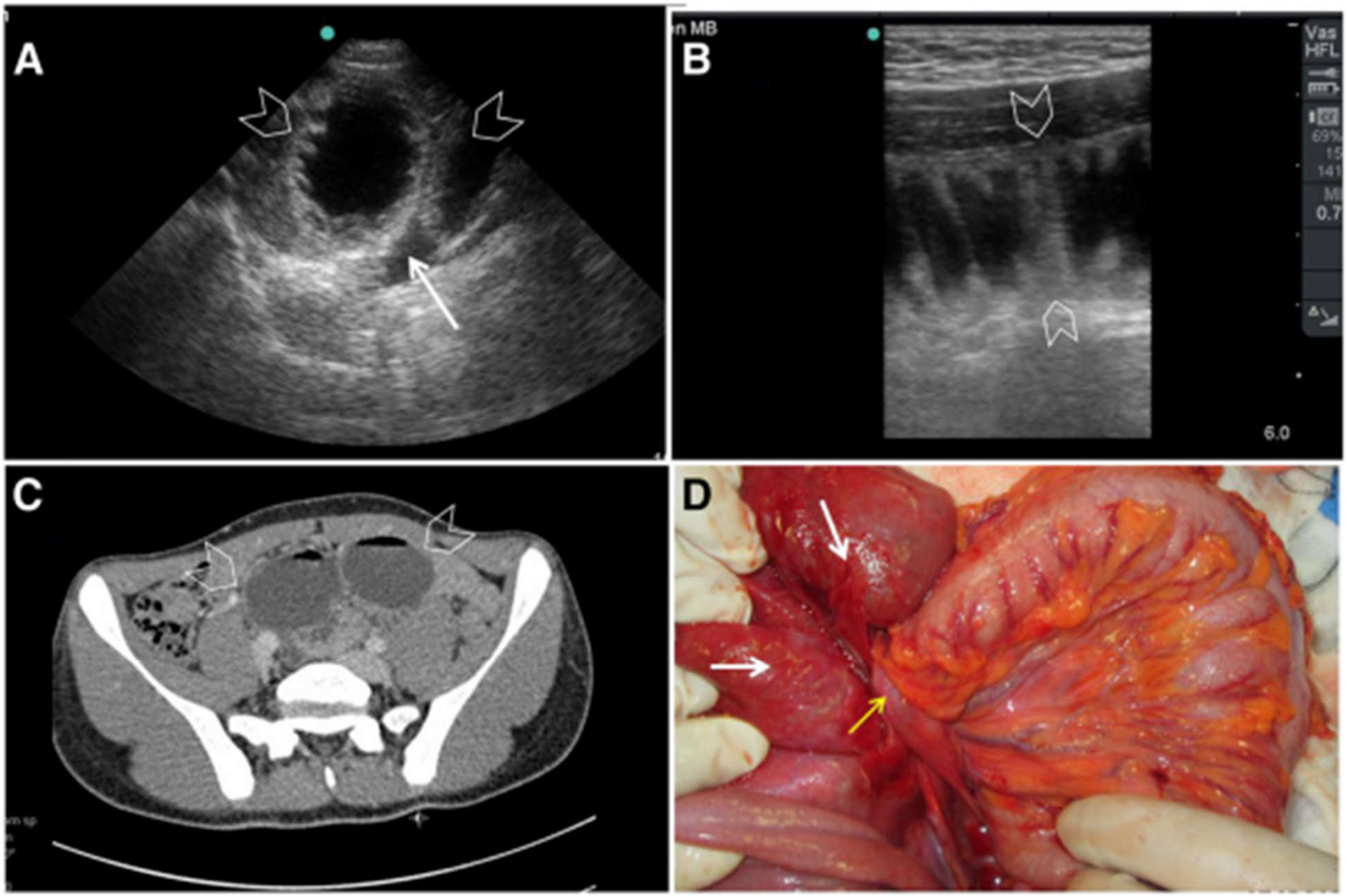

6 A 12-year-old boy presented with abdominal pain and vomiting. On examination, the lower abdomen was not distended, soft, but
el sounds were reduced. POCUS examination revealed two non-functioning jejunal loops (arrowheads) (**a**–**b**) as evidenced by the val
niventes of the loops. Abdominal CT scan confirmed the same findings (**c**). The patient did not respond to conservative management
ded surgery. Laparotomy (**d**) has shown the two jejunal loops (white arrows) obstructed by a congenital fibrous band (yellow arrow)

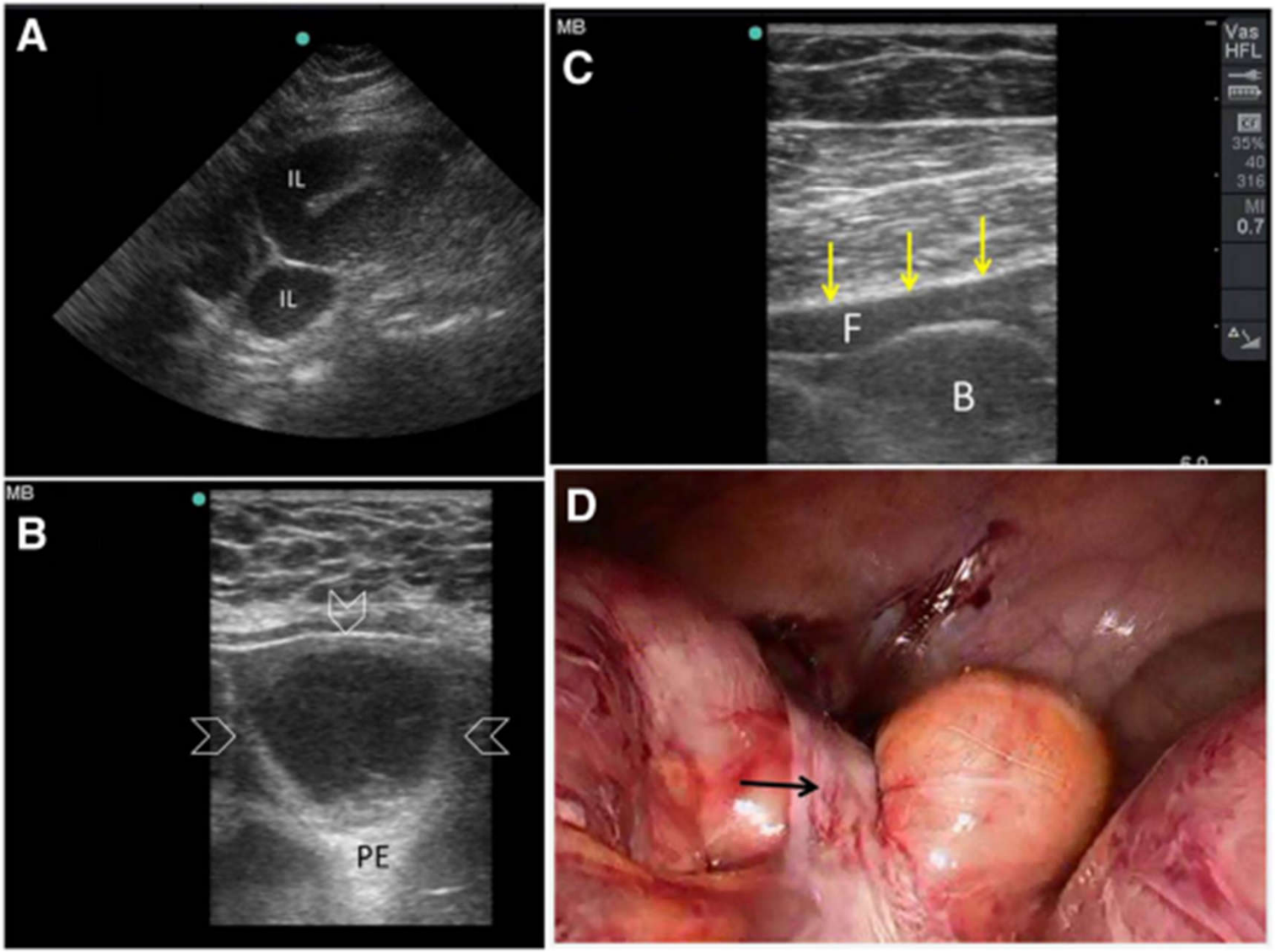

g. 7 A 24-year-old woman presented with 1 day duration of abdominal pain, distension, vomiting, and constipation. She had a caesarian ction 7 months ago. The abdomen was distended, soft, and non-tender. POCUS (**a**) using small print convex array probe (3–5 MHZ) showed tive dilated ileal loops (IL) which was confirmed by the high-frequency linear probe (10–12 Mhz) (arrowheads) (**b**), PE = posterior enhancement tefact. Follow-up POCUS 12 h later using the linear probe (**c**) showed an increased amount of intraperitoneal fluid (F) between the bowel loops) and the abdominal fascia (yellow arrows). The patient underwent laparoscopic surgery (**d**) to release the adhesions (black arrow)

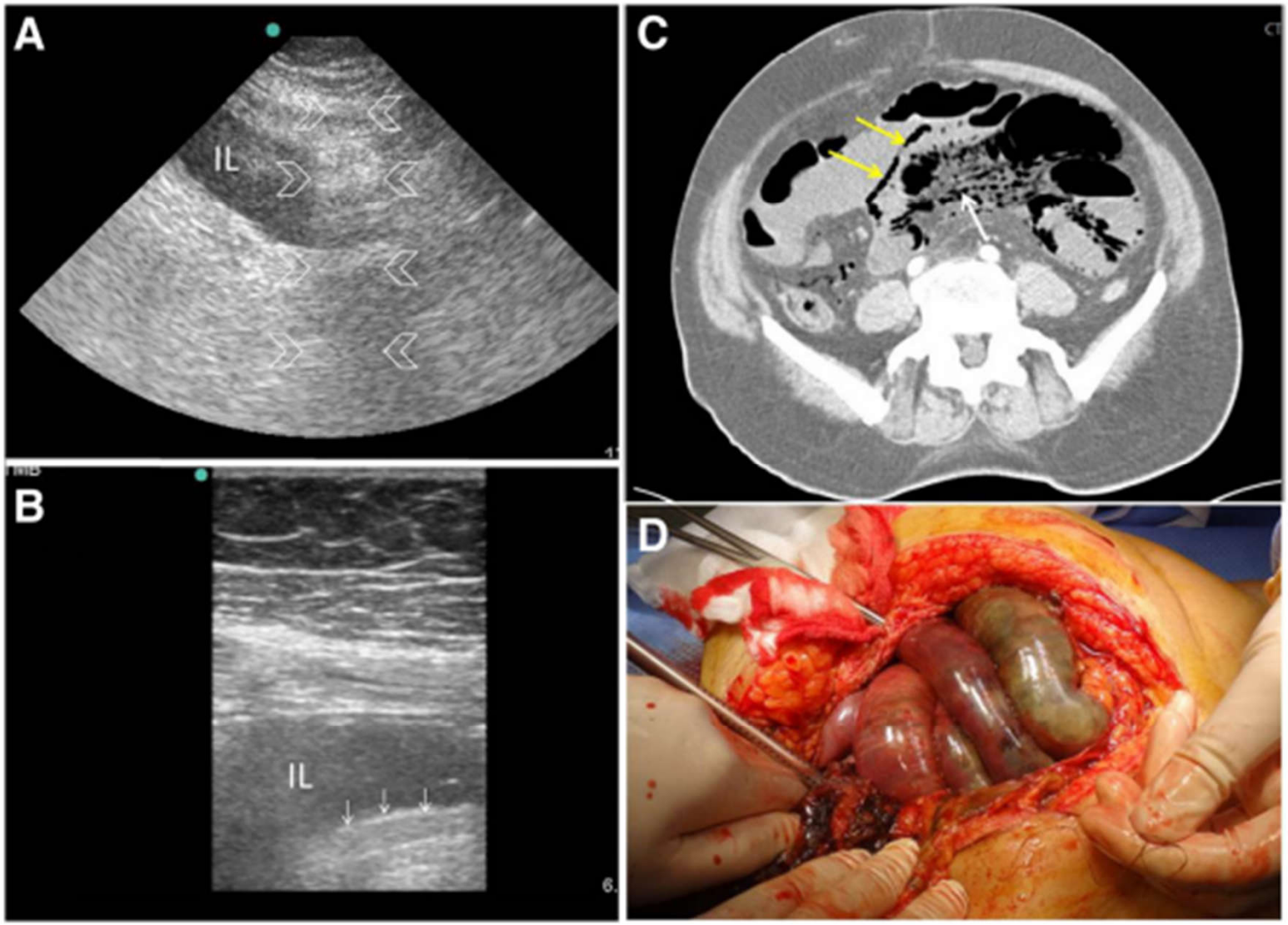

Fig. 8 A 60-year old man who had atrial fibrillation developed abdominal pain of 24 h duration. He had a distended tender abdomen. Bowel sounds were negative. POCUS (**a**) was done using small print convex array probe (3–5 MHz). It was unexpectedly difficult because of obesity and unusual abdominal reverberation artefacts (arrowheads). The ileum (IL) was dilated and non-active. The high-frequency linear probe (10–12 Mhz) (**b**) confirmed these findings and detected gas within the bowel wall shown as tiny white dots (white arrows). CT angiography scan (**c**) showed superior mesenteric artery occlusion with massive bowel ischaemia. The small bowel loops had non-enhancing walls and pneumatosis intestinal (yellow arrows). There was massive gas in the mesenteric vessels (white arrow). Laparotomy confirmed these findings (**d**). Clinical image, Courtes of Dr Hussam Mousa, Department of Surgery, College of Medicine and Health Sciences, UAE University, Al-Ain, United Arab Emirates

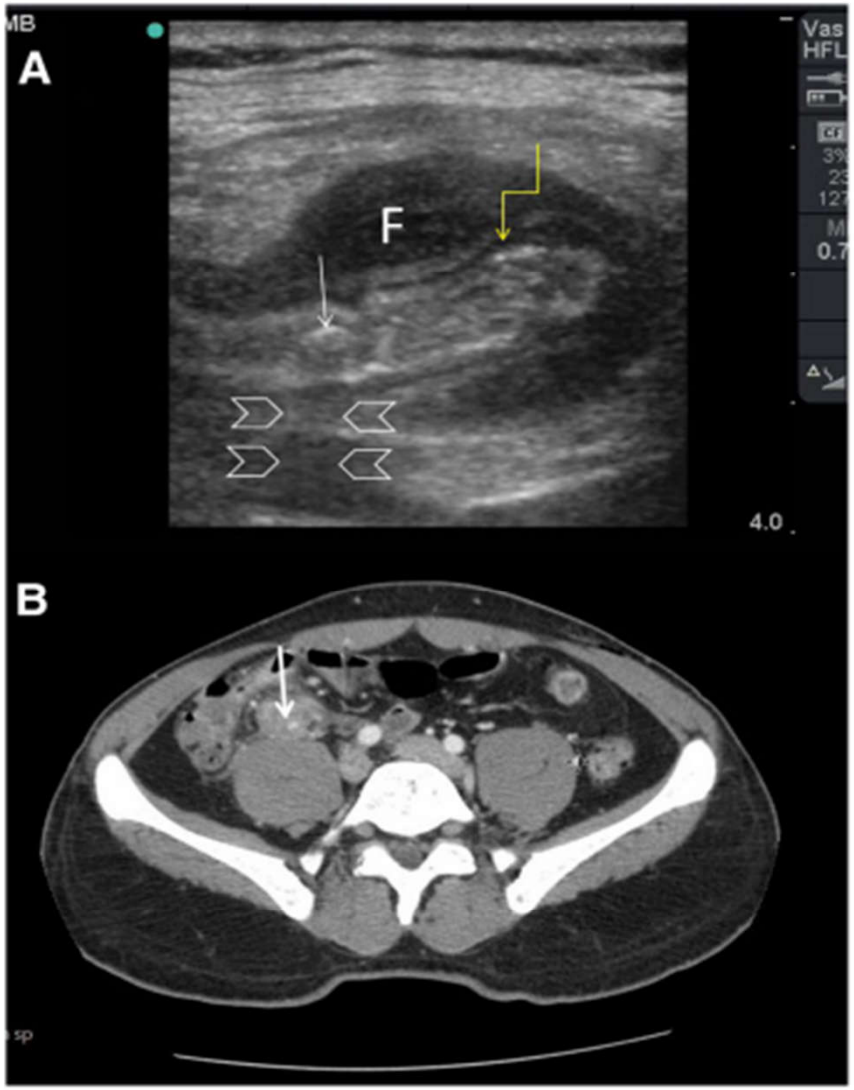

Fig. 9 A 40-year-old man presented complaining of fever and pain in the right iliac fossa of 5 days duration. A hard tender mass was felt in the right iliac fossa. CRP was high. POCUS study (**a**) using a portable ultrasound machine and a high-frequency linear probe has shown a thickened appendicitis with oedema in the muscularis propria (yellow arrow) surrounded by fluid (F). There was a faecolith (white arrow) with a shadow behind it (arrowheads). Abdominal CT scan with intravenous contrast has confirmed the same findings (**b**). Interval appendectomy which was performed two months later confirmed the diagnosis

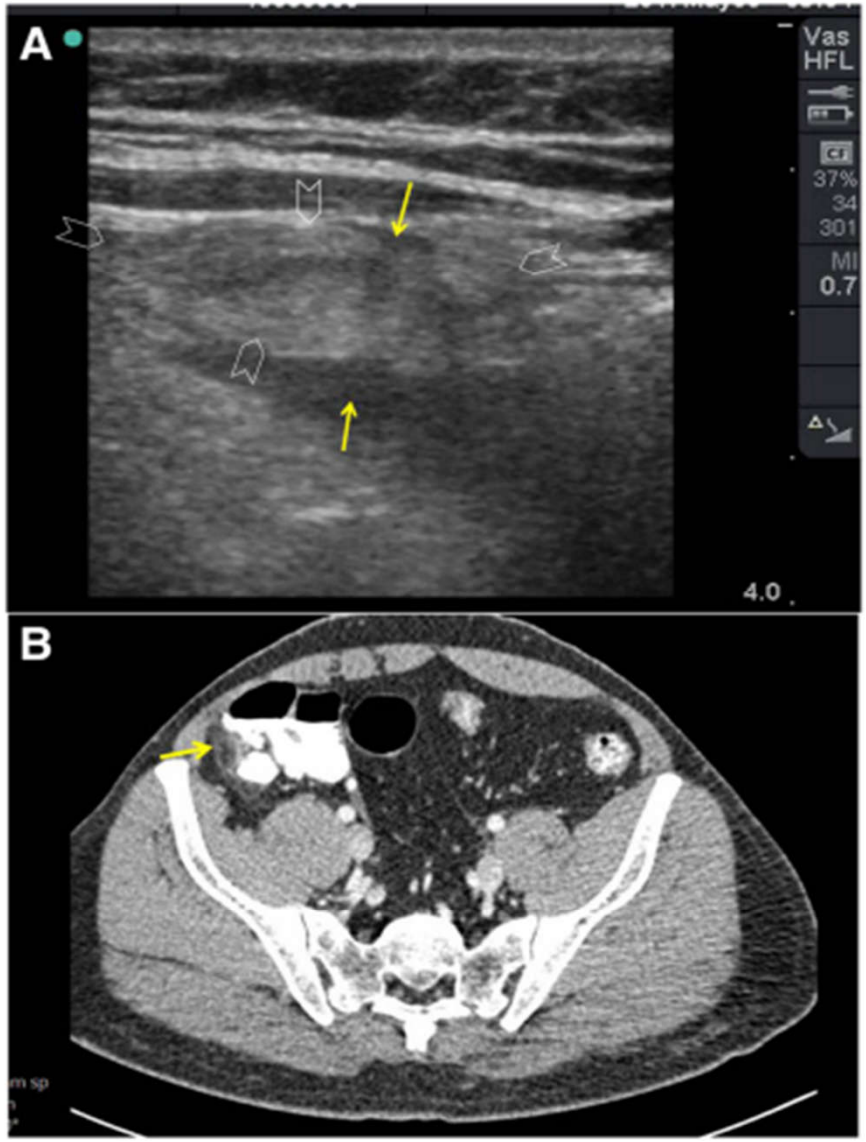

Fig. 10 A 36-year-old man presented with right iliac fossa pain. The patient was afebrile. There was no leukocytosis and C-reactive protein was normal. The abdomen was soft but tender. POCUS (**a**) using a high-frequency linear probe showed a hyperechoic non-compressible ovoid mass adherent to the colonic wall at the maximum tenderness point (arrowheads) which was surrounded by fluid (yellow arrows). Abdominal CT scan with intravenous contrast (**b**) confirmed the diagnosis of epiploic appendagitis (yellow arrow)

Fig. 11 A 32-year-old man presented with left lower q
abdominal pain of 5 days duration. Abdominal examina
a tender mass in the LLQ. The patient had leukocytosis
CRP. POCUS study (**a**) using a portable ultrasound mac
small print convex array probe with a frequency of 3–5
shown a rounded mass (arrowheads). A more detailed
using a high-frequency linear probe showed that the mas
had a rounded folded edge giving it the classical *saw-too*
hypoechoic area represents the muscularis propria (arrow)

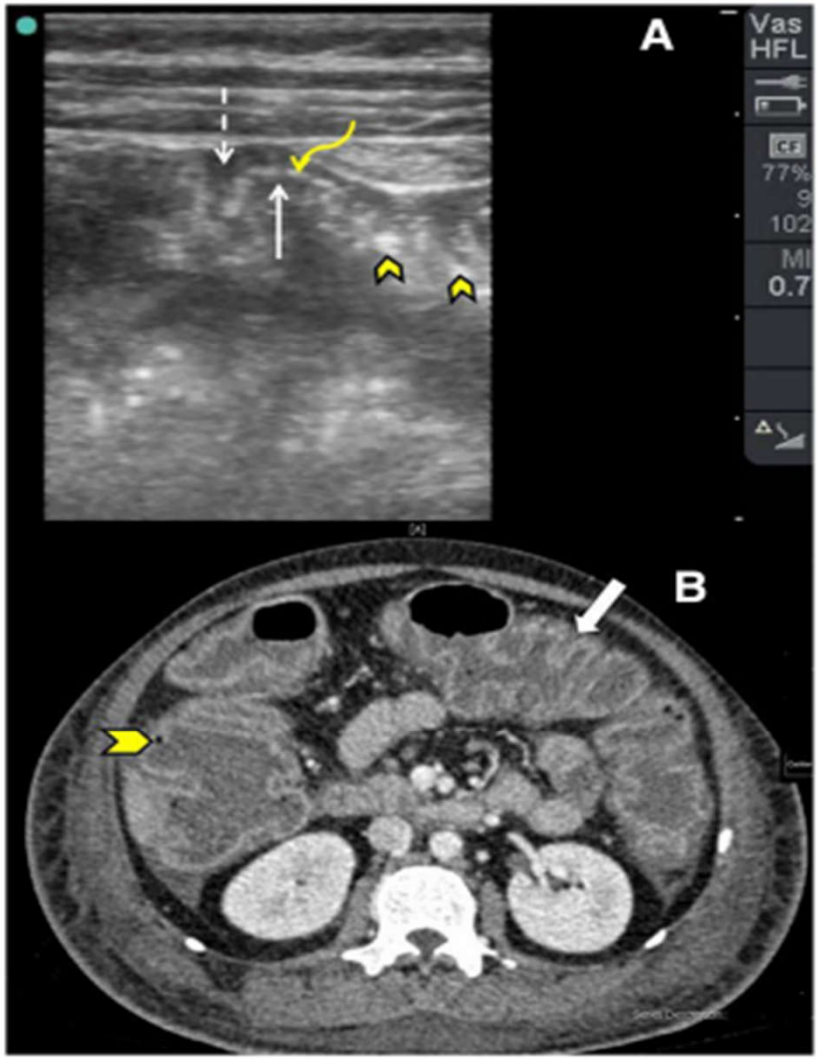

Fig. 12 POCUS study (**a**) using a high-frequency linear probe in multi-trauma patients who developed diarrhoea 2 weeks after starting antibiotic administration. The colonic wall is thickened with three distinct layers, mucosa (white arrow), submucosa (curved yellow arrow), and muscularis propria (interrupted arrow). Hyperechoic lines are seen covering the mucosa (arrowheads). These can be either pseudomembranes or air bubbles. These findings give the classical accordion sign of pseudomembranous colitis. Abdominal CT scan with intravenous contrast (**b**) which was performed at the same time shows the same accordion sign (white arrow). CT scan has the advantage of showing the hyperaemic mucosa with air bubble in the colonic wall (arrowhead)

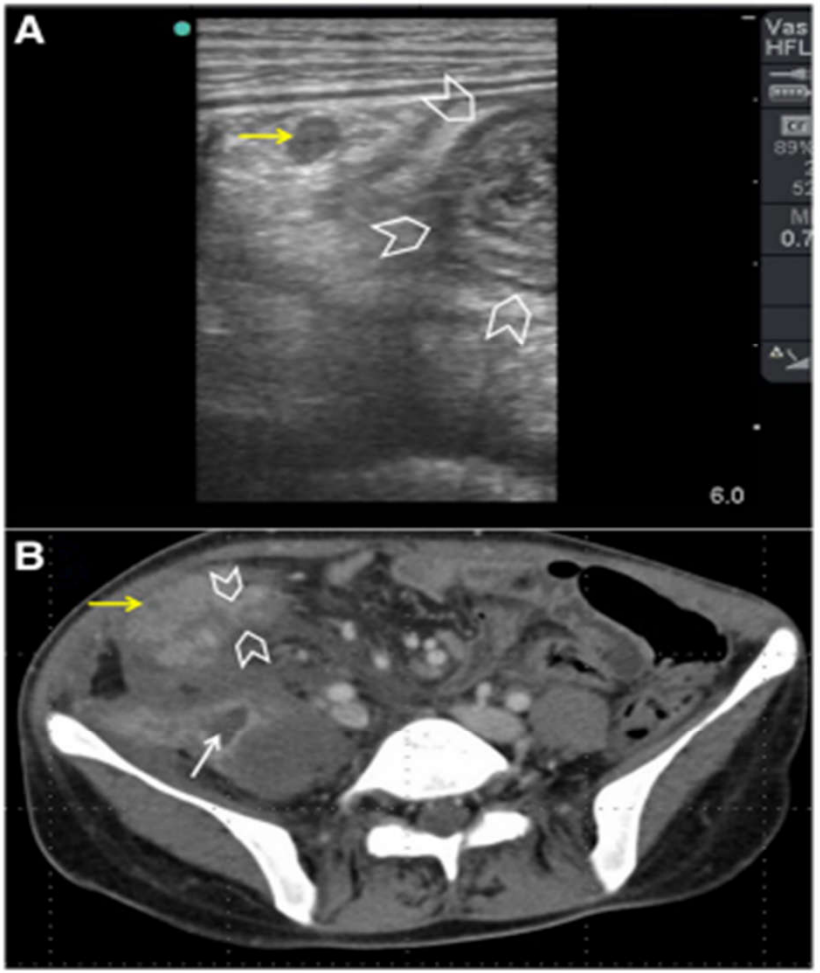

Fig. 13 A 30-year-old woman presented with a tender right iliac fossa mass of 4 months duration. The mass was fixed and hard. POCUS (**a**) using a high-frequency linear probe showed matted thickened inflamed small bowel (arrowheads) and regional lymph nodes (yellow arrow). Abdominal CT scan with intravenous contrast (**b**) confirmed the presence of the thickened bowel (arrowheads) and the enlarged lymph nodes (yellow arrow). There was an ileo-psoas abscess (white arrow). Biopsies through a colonoscopy and an interferon test were non-conclusive. The patient was started on anti-tuberculous treatment as a therapeutic diagnosis

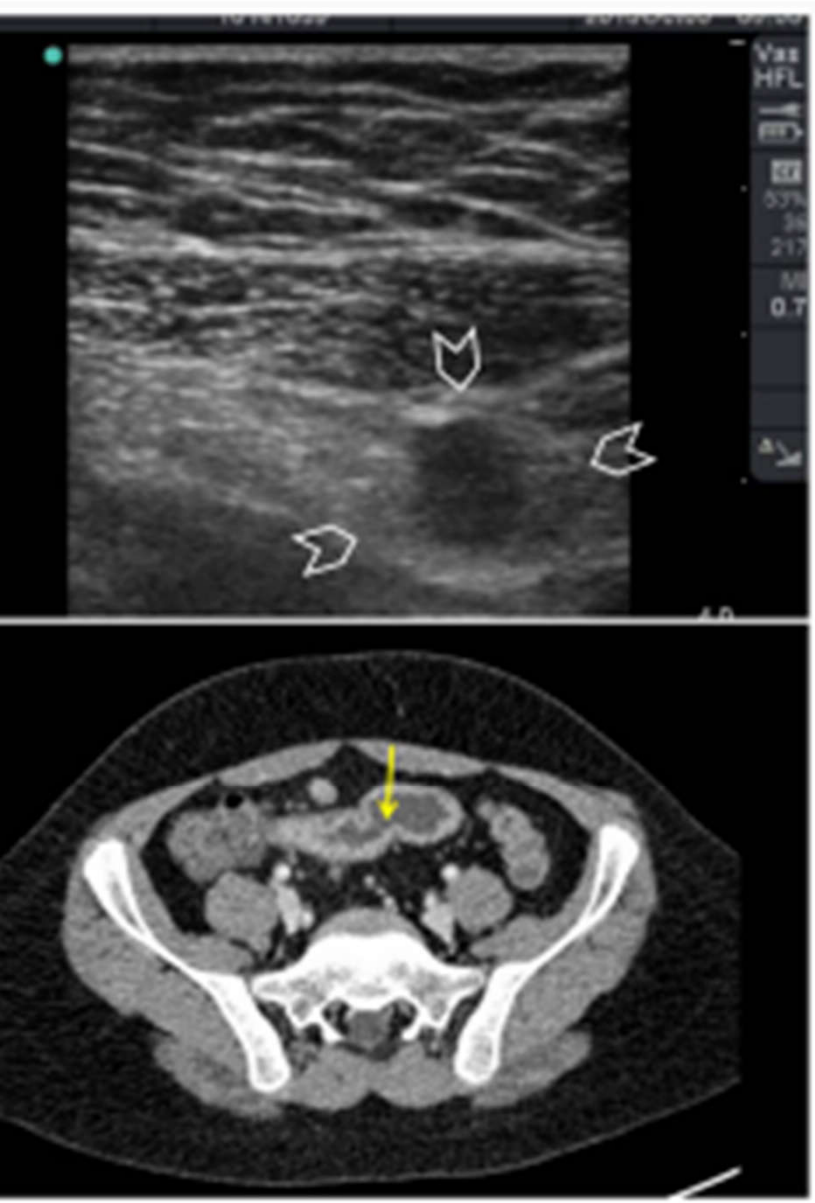

14-year-old boy presented with pain in the right iliac fossa
th duration associated with diarrhoea. His abdomen was
ender at the right iliac fossa. POCUS (**a**) using a high-
linear probe of the right iliac fossa showed a thickened
oic non-compressible small bowel (arrowheads). The bowel
ld not be seen. Crohn's disease was suspected. CT with
us contrast (**b**) showed a thickened constricted terminal
gestive of Crohn's disease (yellow arrow)

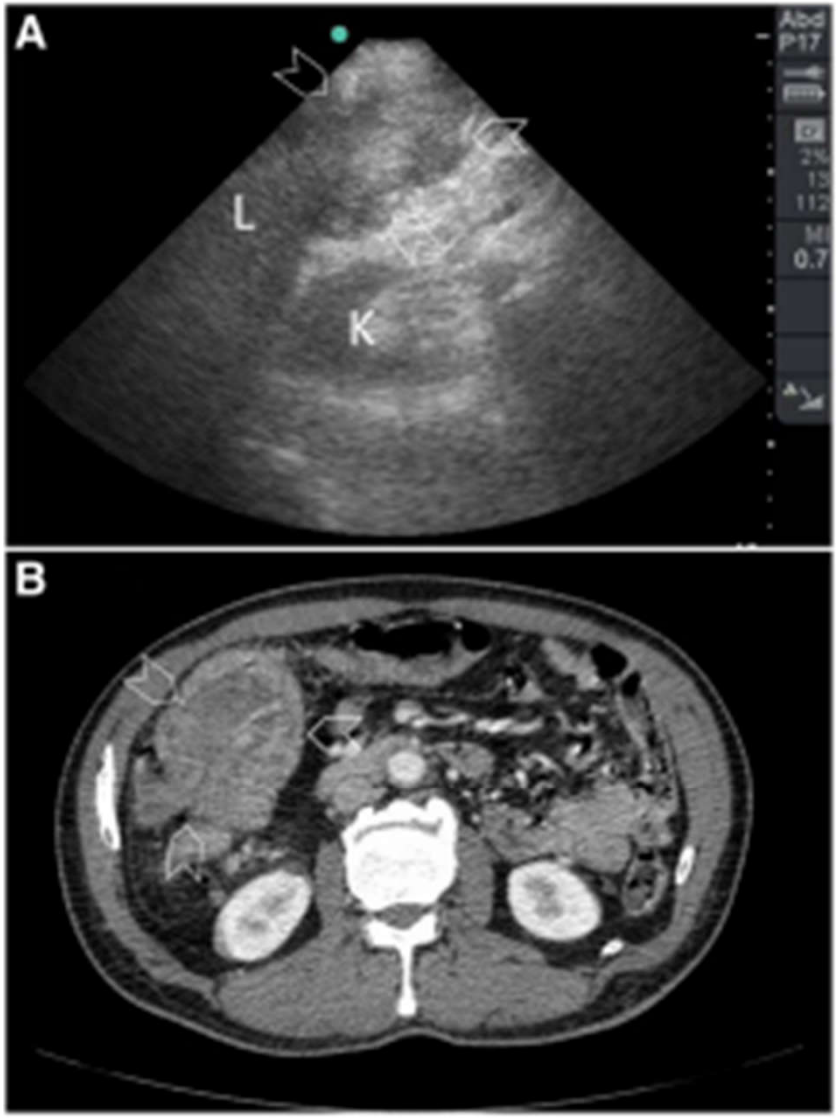

Fig. 15 A 57-year-old man presented with abdominal pain and diarrhoea of 10 days duration. On abdominal examination, there was a mobile mass in the right upper quadrant. The abdomen was soft and not distended. The patient was anemic. POCUS study (**a**) using a portable ultrasound machine and a small print convex array probe having a frequency of 3–5 MHz has shown an irregular mass in the right colon without a lumen just under the liver and 10 cm long (arrowheads). A clinical diagnosis of right colonic malignancy was suspected. CT scan with intravenous contrast (**b**) has shown the same findings (arrowheads). The patient had a right hemicolectomy. The tumour was confirmed to be a poorly differentiated colonic adenocarcinoma. L liver, K kidney

Wiley Online Library

JUM Journal of Ultrasound in Medicine

aium

Review Article | Open Access

Imaging of the Diaphragm Following Cardiac Surgery

Focus on Ultrasonographic Assessment

Vincenzo Rizza MD, Francesco Maranta MD, Lorenzo Cianfanelli MD, Iside Cartella MD, Ottavio Alfieri MD, Domenico Cianflone MD

First published: 26 June 2023 | https://doi.org/10.1002/jum.16291

The authors have no conflicts of interest to report.

Conclusion

Diaphragm dysfunction is a frequent complication aftercardiac surgery which negatively affec patients'clini-cal outcomes. Several techniques can be used to diag-nose diaphragm dysfuncti is an accurate, non-invasive tool to identify and monitor post-operativediaphragm dysfunctio different settings like the CSand the CR Unit. Diaphragm US parameters are alsouseful to opti the ventilatory weaning among theICU patients. Further studies are necessary to establishdef cut-offs for diaphragm dysfunction in spe-cific populations and to define standardized protoc the use of diaphragm US in the clinical practice.

the different diaphragmatic US views. **A**, Intercostal view: high-frequency linear transducer (7–18 MHz) een the seventh and eighth or eighth and ninth ribs along the anterior axillary line. **B**, Anterior subcostal sducer (2–6 MHz) placed in the anterior subcostal region between midclavicular and anterior axillary ency curvilinear transducer (2–6 MHz) placed horizontally under the xiphoid process with the probe ori- e with the anterior abdominal wall. **D**, Posterior subcostal view: low-frequency curvilinear transducer (2– ostal region with the patient in the sitting position.

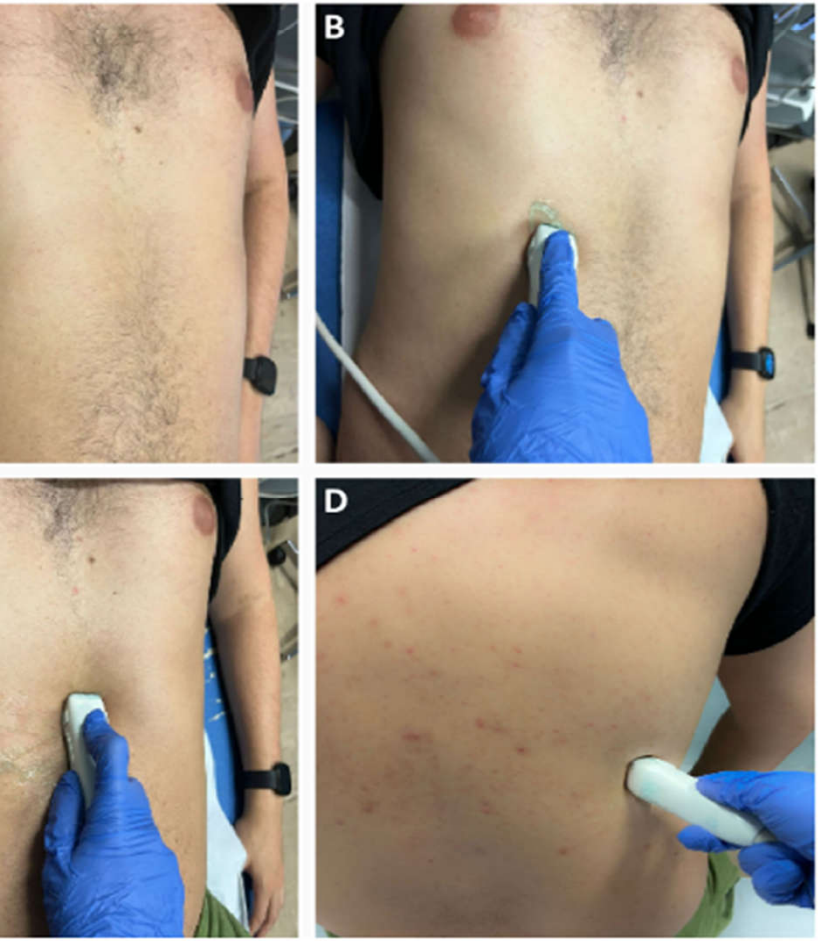

Figure 4. Measurement of the main diaphragmatic US parameters. TF, thickening fraction.